ON THE REFLECTION OF SHORT-CRESTED WAVES IN NUMERICAL MODELS

Michael Brorsen [1] and Jacob Helm–Petersen [1]

Abstract

The paper concerns the reflection performance of so-called 'sponge' layers, which are used to model partially reflecting (porous) structures in a numerical model domain. Various compositions of sponge layers and their performance with respect to wave reflection, main direction of propagation, and directional spreading have been investigated. The numerical model used in this study was a finite difference model based on the time-dependent mild-slope equation. Comparisons are made with reflection measured in physical experiments with short-crested waves. The results obtained so far indicate that in several cases partial reflection of short crested waves can be described satisfactorily in numerical models by use of sponge layers.

Introduction

An accurate modelling of reflection may be of great importance when the wave disturbance in a harbour is estimated by use of a numerical model.

In order to obtain a correct partial reflection from a porous structure under arbitrary wave conditions, it is necessary to set up a 3D numerical model to describe the flow in the porous structure. This would lead to a computational effort that normally cannot be afforded in a practical investigation of wave disturbance in a harbour.

Models based on depth integrated flow equations are nearly always applied in practical investigations of wave fields in order to reduce the computational effort. Typical examples of depth integrated equations are Boussinesq equations or mild-slope equations.

In models based on Boussinesq equations it is rather easy to model the depth integrated flow in a porous structure with vertical front. Terms describing the

[1]Hydraulics & Coastal Engineering Laboratory, Dept. of Civil Engineering
Aalborg University, Sohngaardsholmsvej 57, DK–9000 Aalborg

dissipation are included in the governing equations, and dissipation as well as reflection can be modelled rather accurately in such numerical models, at least in case of head on waves (Madsen and Warren, 1984). A major drawback of these models is the necessary substantial computational effort, and some 'tuning' is normally still necessary to obtain a correct reflection coefficient.

Models based on mild-slope equations may demand much less computational effort, especially if partial reflection could be modelled by implementation of a simple boundary condition for the surface elevation or the velocity potential at the structure. With such a type of boundary condition one has to specify the reflection coefficient beforehand and this demands an estimate of the yet unknown wave steepnees. In principle an iterative approach is therefore necessary.

Furthermore, it is not straightforward to obtain an analytical boundary condition which combines good performance with respect to the angle of incidence of the waves and easiness of implementation into the numerical model see e.g. Behrendt (1986) and Dingemans (1997).

The present paper concerns the reflection performance of so-called 'sponge' layers, which are used to model partially reflecting (porous) structures in the numerical model domain. The applied sponge layer technique was first described by Larsen and Dancy (1983). This technique is very easy to implement into finite difference models and has been used extensively to model open boundaries, i.e. boundaries where the goal is no reflection at all.

Various compositions of sponge layers and their performance with respect to wave reflection, main direction of propagation, and directional spreading have been investigated with models based on the finite difference method.

Attention has also been paid to the effects due to the discretization of an oblique structure with straight front in a finite difference model. Here an oblique structure means a structure, where the front of the structure is not aligned with a grid line in the model domain. For such a structure the straight front will be discretized into shorter pieces in the numerical model which might influence the reflection from the structure. Comparisons are made with reflection measured in physical experiments with short-crested waves (Helm-Petersen, 1994).

Numerical model

The numerical model was based on the time-dependent mild-slope equation, see e.g. Kirby et al. (1992) and Dingemans (1997). In this equation the vertical dependence is extracted from the velocity potential $\phi(x, y, z, t)$ according to

$$\phi(x, y, z, t) = f(z, h) \cdot \varphi(x, y, t) \tag{1}$$

where

$$f(z, h) = \frac{\cosh k(z+h)}{\cosh kh} \tag{2}$$

Here $\varphi(x, y, t)$ is the velocity potential at $z = 0$, h is the local still water depth, k is the local wave number and z a vertical co-ordinate.

Assuming small variations in the seabed topography (mild slopes) and first order wave theory leads to the model equations

$$\eta = -\frac{1}{g}\varphi_t \tag{3}$$

and

$$\eta_t + \frac{\partial}{\partial x}(A\varphi_x) + \frac{\partial}{\partial y}(A\varphi_y) - B\varphi = 0 \tag{4}$$

where

$$A(x,y) = \frac{1}{2k}\left[1 + \frac{2kh}{\sinh(2kh)}\right]\tanh(kh) = \frac{c\,c_g}{g} \tag{5}$$

$$B(x,y) = \frac{k}{2}\left[1 - \frac{2kh}{\sinh(2kh)}\right]\tanh(kh) = \frac{\omega^2 - k^2\,c\,c_g}{g} \tag{6}$$

and ω is the circular frequency, c is the phase velocity and c_g is the group velocity.

If equation (3) is substituted into equation (4) the result is the hyperbolic time-dependent mild-slope equation. This equation is able to handle refraction, shoaling, diffraction and reflection of linear, irregular waves provided that the sea state can be described by a narrow frequency spectrum (Dingemans, 1997) with a dominant carrier frequency $\bar{\omega}$.

In this study the numerical solution was based on an explicit finite difference discretization of equation (3) and equation (4). The computational domain was divided into quadratic boxes, and central differences were used for spatial as well as time derivatives. Both η and φ were calculated at the center of each box (but at different new time levels, $(n+1/2)\,\Delta t$ and $(n+1)\,\Delta t$, respectively) from the discretized equations:

$$\begin{aligned}\frac{\eta_{i,j}^{n+\frac{1}{2}} - \eta_{i,j}^{n-\frac{1}{2}}}{\Delta t} \simeq\ & B_{i,j}\varphi_{i,j}^n \\ & -\frac{A_{i+1,j} - A_{i-1,j}}{2\Delta x}\cdot\frac{\varphi_{i+1,j}^n - \varphi_{i-1,j}^n}{2\Delta x} \\ & -A_{i,j}\frac{\varphi_{i-1,j}^n - 2\varphi_{i,j}^n + \varphi_{i+1,j}^n}{(\Delta x)^2} \\ & -\frac{A_{i,j+1} - A_{i,j-1}}{2\Delta y}\cdot\frac{\varphi_{i,j+1}^n - \varphi_{i,j-1}^n}{2\Delta y} \\ & -A_{i,j}\frac{\varphi_{i,j-1}^n - 2\varphi_{i,j}^n + \varphi_{i,j+1}^n}{(\Delta y)^2}\end{aligned} \tag{7}$$

$$\eta_{i,j}^{n+\frac{1}{2}} = -\frac{1}{g}(\varphi_t)_{i,j}^{n+\frac{1}{2}} \simeq -\frac{1}{g}\frac{\varphi_{i,j}^{n+1} - \varphi_{i,j}^n}{\Delta t} \tag{8}$$

In each time step $\eta_{i,j}^{n+1/2}$ was first calculated by equation (7) and then $\varphi_{i,j}^{n+1}$ was calculated by equation (8).

Fully reflective boundaries were modelled by forcing the flow to be zero between the two boxes on each side of the boundary. This was obtained by setting the values of φ at the two boxes to be equal.

Partially reflective boundaries were modelled by use of sponge layers. A reduction factor $\mu < 1$ is specified for each box in the sponge layer. In each time step the surface elevation, η, was calculated in each box within the entire domain. Hereafter, also at each time step, the η-values in sponge layers are multiplied by the corresponding μ-factors. Thus energy was extracted from the system. The width (no of boxes) of a sponge layer, denoted W_s, and the μ-values corresponding to a desired reflection coefficient were found by trial and error for head on waves in a numerical wave flume.

The factor μ was found from the expression

$$\mu = \frac{1}{(a-1)(\frac{n}{N})^b + 1} \tag{9}$$

where n (the type of the sponge box) is an integer between 1 and N, a and b are constants. Open boundaries were modelled by sponge layers where the type n was varied linearly from the beginning of the sponge layer to the boundary of the computational domain. The reflection coefficient from such a layer was typically only a few percent if the width of the sponge layer was approximately 2 times the wave length corresponding to the peak frequency of a sea state.

A single summation wave generation model (Miles, 1989) was applied to generate the short crested sea state. Hence each wave component had a unique frequency, whereas several wave components were travelling in the same direction. This can be expressed as

$$\eta(x,y,t) = \sum_{l=1}^{L}\sum_{m=1}^{M} A_{lm}\cos(\omega_{lm}t - k_{lm}(x\cos\theta_m + y\sin\theta_m) + \phi_{lm}) \tag{10}$$

where

$$\begin{aligned} \omega_{lm} &= 2\pi f_{lm} \\ &= 2\pi(M(l-1)+m)\Delta f + 2\pi f_{min} && (11) \\ A_{lm} &= \sqrt{2S(f_{lm})H(f_{lm},\theta_m)M\Delta f\Delta\theta} && (12) \\ \theta_m &= (m-1)\Delta\theta - \theta_{max} && (13) \end{aligned}$$

ϕ_{lm} is a random phase, $S(\cdot)$ and $H(\cdot)$ are the wave energy spectrum and the directional spreading function, respectively.

The waves were generated in the numerical model by the method described in Larsen and Dancy (1983) by adding or removing volume along a gridline, referred to as the wave generation line. In order to generate a single wave component

$$\begin{aligned} \eta_I &= a\sin(kx' - \omega t + \varphi) && (14) \\ &= a\sin(k\cos\theta x^* + k\sin\theta x^* - \omega t + \varphi) && (15) \end{aligned}$$

travelling in the direction θ, see Figure 1, the necessary volume to be added at each generation box at each time step was calculated from equation

$$\Delta\eta = \frac{2\,c_e\eta_I\cos\theta\Delta t}{\Delta x} \tag{16}$$

where c_e is the energy velocity defined (Suh et al., 1997) as

$$c_e = \bar{c}_g\frac{\bar{\omega}}{\omega}\sqrt{1+\frac{\bar{c}}{\bar{c}_g}\left((\frac{\omega}{\bar{\omega}})^2-1\right)} \tag{17}$$

Here the overbar is associated with the applied carrier frequency.

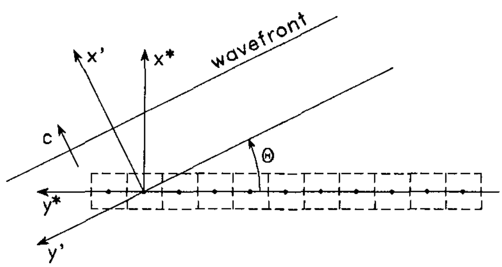

Figure 1: Definition of parameters.

Analysis of data

Directional spectra were estimated by use of the software package PADIWA (1997), which is based on the Bayesian Directional Spectrum Estimation Method - BDM (Hashimoto and Kobune, 1988). This method estimates the spreading function $H(f,\theta)$, and the directional spectrum $S(f,\theta)$ was found from

$$S(f,\theta) = H(f,\theta)\,S(f) \tag{18}$$

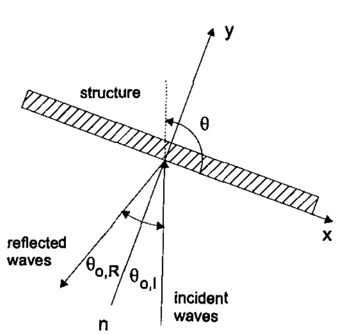

Figure 2: Definition sketch of propagation angles.

From Figure 2 it is seen that waves propagating in directions between 0° and 180° were incident waves, and waves propagating in directions between 180° and 360° were reflected waves. Having estimates of $H(f,\theta)$ in K directions at each frequency, the main propagation directions for incident and reflected waves, see Figure 2, were found from

$$\theta_{o,I}(f) = \sum_{k=1}^{K/2} \theta_k\, H(f,\theta_k)\,\Delta\theta - 90^\circ \tag{19}$$

$$\theta_{o,R}(f) = 270^\circ - \sum_{k=K/2+1}^{K} \theta_k\, H(f,\theta_k)\,\Delta\theta \tag{20}$$

and the variances of the directional spreading functions from

$$\sigma^2_{\theta,I}(f) = \sum_{k=1}^{K/2} (\theta_k - \theta_{o,I}(f))^2\, H(f,\theta_k)\,\Delta\theta \tag{21}$$

$$\sigma^2_{\theta,R}(f) = \sum_{k=K/2+1}^{K} (\theta_k - \theta_{o,R}(f))^2\, H(f,\theta_k)\,\Delta\theta \tag{22}$$

The frequency dependent reflection coefficient (defined as the ratio between wave heights) was found from

$$R(f) = \sqrt{\frac{S_R(f)}{S_I(f)}} \tag{23}$$

and the total reflection coefficient from

$$C_R = \sum \frac{S_I(f) + S_R(f)}{\sum[S_I(f) + S_R(f)]}\, R(f) \tag{24}$$

Numerical simulations

In all simulations the following setup was applied:

- computational domain : 120×208 boxes
- box size : $dx = dy = 0.125$ m
- water depth : $h = 0.61$ m
- Jonswap frequency spectrum ($\gamma = 3.3$), significant wave height $H_s = 0.10$ m and peak period $T_p = 1.5$ secs. Energy outside the frequencies $0.66\, f_p$ and $2\, f_p$ was cut off
- Mitsuyasu spreading function i.e.

  $H(f,\theta) = const \cdot \cos^{2s}(\frac{\theta-\theta_o}{2})$ with $s = 15$ ($\Leftrightarrow \sigma_{\theta,I}(f) = 20°$)

- time step : $dt = 0.05$ sec
- short-crested sea: 220 wavelets
  (20 frequency bands ($L = 20$) each with 11 directions ($M = 11$))
- the sponge layer coefficients were calculated by equation (9) with $a = 1.3$, $b = 1.8$ and $N = 50$.

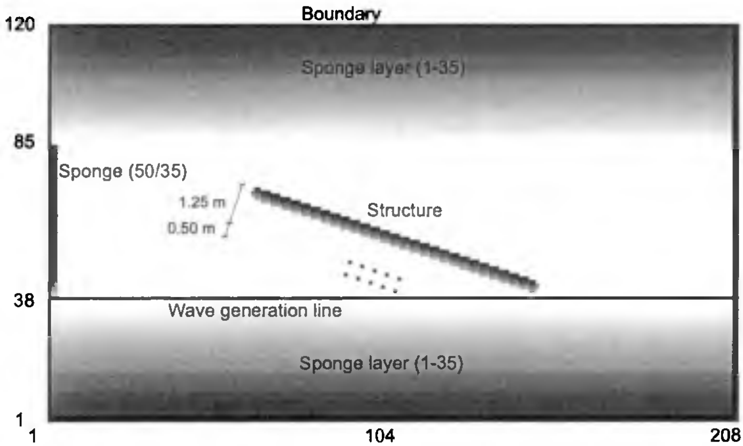

Figure 3: Model setup. Structure with stepped front (1:3), $C_R \approx 55\%$.

Different types and placement of structures were investigated, but the wave generation line and the 2 fully absorbing sponge layers were in all simulations situated as shown in Figure 3. In case of oblique structures an additional sponge layer with $W_s = 2$ and types 50 and 35 was applied at the left boundary of the domain.

In all simulations surface elevation time series were sampled at 10 positions in a 0.5 m×0.5 m grid placed parallel with the front of the actual structure at a distance of 1.25 m, see Figure 3. These time series provided the data for the reflection analysis. The elevation time series were sampled with a frequency of 10 Hz, i.e. every second time step and the duration of each time series was 18 minutes.

The applied setup of measuring positions is not considered optimal, but was chosen in order to get the same setup which was used in similar physical experiments (Helm-Petersen, 1994). In these physical experiments reflection coefficients from a breakwater with a vertical, porous front were determined by use of the same type of analysis applied in the present numerical simulations.

The estimation of the directional spectrum was based on subseries having a duration of 25.6 secs corresponding to a spectral resolution of $\Delta f = 0.039$ Hz. The directional resolution was chosen to 5° corresponding to $K = 72$ directions.

Structures with straight front

In those cases the structure was parallel with the wave generation line. The following reflection conditions were simulated:

- fully reflective front
- partially reflective front, $C_R \approx 85$ %, corresponding to a sponge layer with $W_s = 1$ and $n = 20$ or $\mu = 0.95$
- partially reflective front, $C_R \approx 55$ %, corresponding to a sponge layer with $W_s = 3$ and $n = 20, 25, 35$ corresponding to $\mu = 0.95, 0.92, 0.86$

The results from these simulations are shown in Figures 4 – 7.

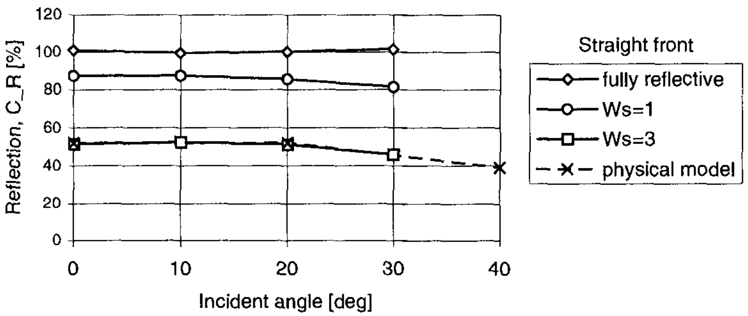

Figure 4: Reflection coefficients. Numerical models with *straight* front and physical model (Helm-Petersen, 1994).

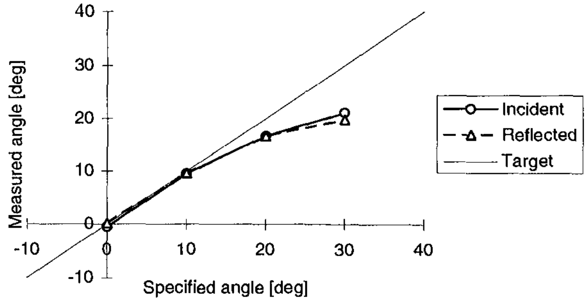

Figure 5: Main propagation angles. Numerical model with *straight* front, $C_R = 100\%$.

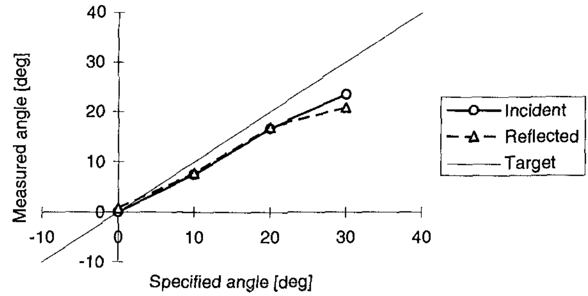

Figure 6: Main propagation angles. Numerical model with *straight* front, $C_R \approx 85$ %, $W_s = 1$.

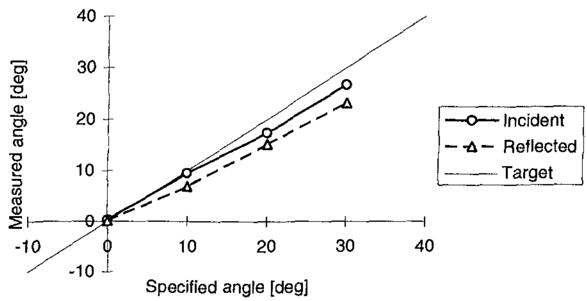

Figure 7: Main propagation angles. Numerical model with *straight* front, $C_R \approx 55$ %, $W_s = 3$.

Structures with stepped front

The oblique structures were forming angles of 9.5° (1:6), 18.4° (1:3) or 26.6° (1:2), respectively, with the computational grid. Hence the discretized front of the models were stepped. The model setup for a structure forming an angle of 18.4° (1:3) with the computational grid is shown in Figure 3. The following conditions were simulated for the three oblique structures:

- fully reflective front.
- partially reflective front, $C_R \approx 55$ %, $W_s = 3$.

The setup of the sponge layers are shown in Figures 8–9, and the results from these simulations are shown in Figures 10 –14.

Discussion of results

For a structure having the front aligned with a grid line in the model domain it was found that sponge layers provide a very reasonable reflection of short-crested

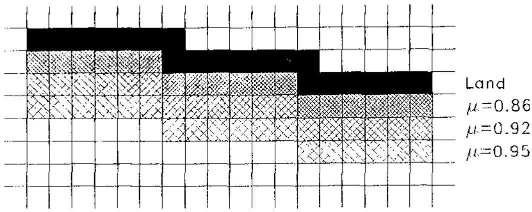

Figure 8: Structure with stepped front (1:6), $C_R \approx 55$ %, $W_s = 3$.

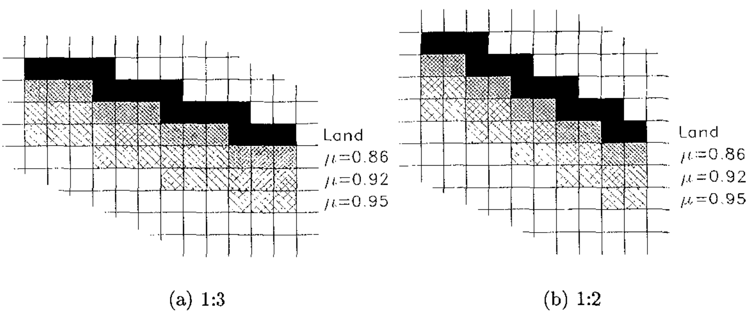

Figure 9: Structures with stepped front, $C_R \approx 55$ %, $W_s = 3$.

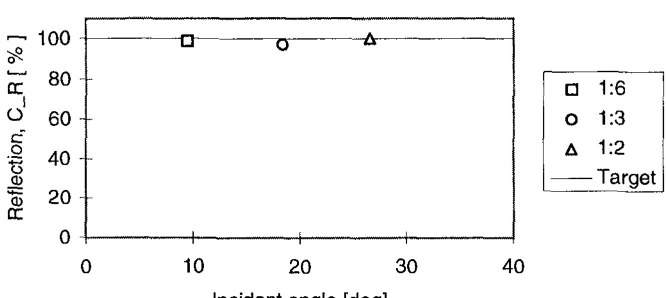

Figure 10: Reflection coefficients. Structures with *stepped* front, fully reflective.

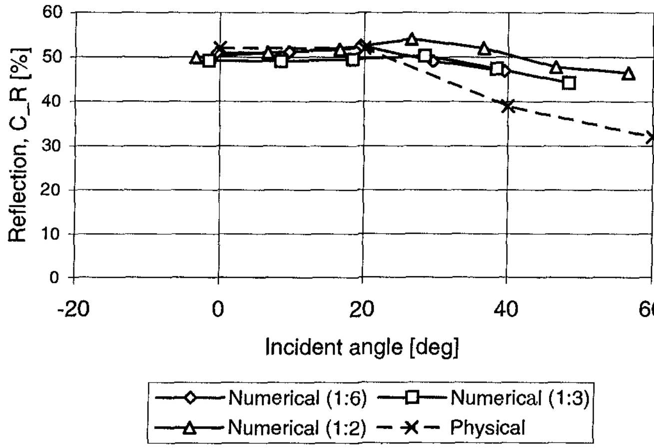

Figure 11: Reflection coefficients. Structures with *stepped* front, $W_s = 3$.

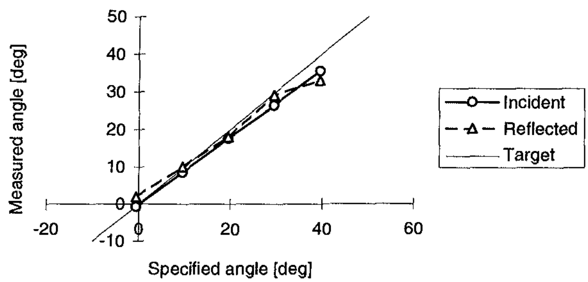

Figure 12: Main propagation angles. Structure with *stepped* front (1:6), $C_R \approx 55$ %, $W_s = 3$.

waves. The variation of the total reflection coefficient C_R with the angle of incidence (main propagation direction) was the same in the numerical and in the physical model in case of a partially reflective front, see Figure 4. Furthermore the main propagation directions of the waves was reflected into directions corresponding to Snell's law, see Figures 5–7. This was also found in the physical experiments. Some deviation between the specified and measured main incident angles are seen for angles larger than 20-30°. In the numerical simulations it was only possible to generate wavelets propagating at angles of approximately 65° from the line of generation and therefore the directional spectrum had to be truncated at angles where considerable energy was present. This might be the main cause to the deviation between the specified and measured main incident angles.

Also in case of oblique structures with a straight front discretized into a stepped front it was found that sponge layers provide a very reasonable reflection of short-crested waves. The total reflection coefficient C_R was modelled correctly op to

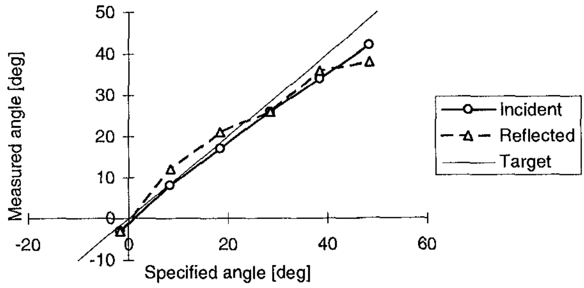

Figure 13: Main propagation angles. Structure with *stepped* front (1:3), $C_R \approx 55$ %, $W_s = 3$.

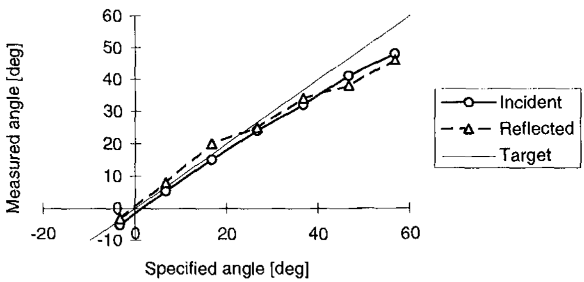

Figure 14: Main propagation angles. Structure with *stepped* front (1:2), $C_R \approx 55$ %, $W_s = 3$.

approximately 20°'s angle of incidence (main propagation direction) in the numerical model. For larger angles the variation of C_R in the numerical simulations had the correct trend, but C_R-values from numerical simulations were somewhat larger than the corresponding C_R-values from the physical experiments, see Figure 11. The main propagation direction of the waves was also in case of stepped fronts reflected into directions corresponding to Snell's law, see Figures 12–14. Due to the oblique structure larger angles of incidence could be obtained, but also in these simulations some deviations between specified and measured main incident angles were seen. Average values of the relative directional spreading, defined as $\sigma_{rel} = \sigma_{\theta,R}/\sigma_{\theta,I}$, are shown in Table 1. It is seen that simulations with partially reflective structures having $C_R \approx 55\%$ typically had a relative spreading $\sigma_{rel} \approx 1.25$. A relative spreading larger than one is to be expected for a partially reflective structure, and in physical experiments with vertical fronts having $C_R \approx 55\%$ (Helm–Petersen, 1994) $\sigma_{rel} \approx 1.20$ was found.

Conclusions

The 3D reflection performance of sponge layers applied in numerical models has been investigated considering short-crested waves. In general the results from the numerical simulations compare well to results from physical experiments carried

Width of layer W_s	type of front	Reflection coeff. C_R [%]	Relative spreading $\sigma_{rel} = \frac{\sigma_{\theta,R}}{\sigma_{\theta,I}}$
0	straight	100	1.00
1	straight	85	1.05
3	straight	55	1.33
3	stepped (1:6)	55	1.18
3	stepped (1:3)	55	1.24
3	stepped (1:2)	55	1.19

Table 1: *Relative directional spreading.*

out with caissons having perforated vertical fronts, and it is found that appropriate 3D reflection can be obtained with respect to the total reflection coefficient, main propagation direction of the reflected waves and the relative directional spreading.

Acknowledgements

Part of this work has been carried out under the frame work programme *Marine Techniques 2* (Marin Teknik 2) of the Danish Technical Research Council.

References

Behrendt, L. (1985), A finite element model for water wave diffraction including boundary absorption and bottom friction, ISVA Series Paper 37, Technical University of Denmark.

Dingemans, M. W. (1997), Water Wave Propagation over Uneven Bottoms, Part 1, Advanced Series on Ocean Engineering–Volume 13, World Scientific.

Hashimoto, N. and K. Kobune (1988). Directional spectrum estimation from a Bayesian approach. In Proc. 21st International Conference on Coastal Engineering, Malaga, Spain, pp. 62-76.

Helm–Petersen, J. (1994). Reflection from caissons in multidirectional seas. In *3rd MCS Project Workshop, MAS2-CT92-0047, Monolithic (vertical) Coastal Structures.*

Kirby, J. T., C. Lee and C. Rasmussen (1992), Time-Dependent Solutions of the Mild–Slope Wave Equation, Proc. 23rd International Conference on Coastal Engineering, Venice, Italy, pp. 391-404.

Larsen, J. and H. Dancy (1983). Open boundaries in short wave simulations - a new approach. Coastal Engineering, Volume 7, pp. 285-297.

Madsen, P. A. and I .R. Warren (1984). Performance of a numerical short wave model. Coastal Engineering, Volume 8, pp. 73-93.

Miles, M. D. (1989). A note on directional random wave synthesis by the single-summation method, XXIII Congress, IAHR, Ottawa, Canada, vol. C, pp. 243-250.

PADIWA (1997). A Package for Directional Wave Analysis. Hydraulics and Coastal Engineering Laboratory, Aalborg University.

Suh, K. D., C. Lee and W. S. Park (1997). Time dependent equations for wave propagation on rapidly varying topography. Coastal Engineering, Volume 32, pp. 91-117.